



Schisandrin A enhances the cytotoxicity of doxorubicin by the inhibition of nuclear factor-kappa B signaling in a doxorubicin-resistant human osteosarcoma cell line

Journal:	<i>RSC Advances</i>
Manuscript ID:	RA-ART-11-2014-014324.R1
Article Type:	Paper
Date Submitted by the Author:	22-Dec-2014
Complete List of Authors:	Xia, Yuan-Zheng; China Pharmaceutical University, Department of Natural Medicinal Chemistry Yang, Lei; China Pharmaceutical University, Department of Natural Medicinal Chemistry Wang, Zhen-Dong; China Pharmaceutical University, Department of Natural Medicinal Chemistry Guo, Chao; China Pharmaceutical University, Department of Natural Medicinal Chemistry zhang, chao; China Pharmaceutical University, Department of Natural Medicinal Chemistry Geng, Ya-Di; China Pharmaceutical University, Department of Natural Medicinal Chemistry Kong, Ling-Yi; China Pharmaceutical University, Department of Natural Medicinal Chemistry

Schisandrin A enhances the cytotoxicity of doxorubicin by the inhibition of nuclear factor-kappa B signaling in a doxorubicin-resistant human osteosarcoma cell line¹

Yuan-Zheng Xia, Lei Yang, Zhen-Dong Wang, Chao Guo, Chao Zhang, Ya-Di Geng and Ling-Yi Kong*

¹State Key Laboratory of Natural Medicines, Department of Natural Medicinal Chemistry, China Pharmaceutical University, 24 Tong Jia Xiang, Nan Jing 210009, People's Republic of China

*Corresponding Author: Ling-Yi Kong

Full address: State Key Laboratory of Natural Medicines, Department of Natural Medicinal Chemistry, China Pharmaceutical University, 24 Tongji Xiang, Nanjing 210009, People's Republic of China

Tel/Fax: +86 25 8327 1405.

E-mail: cpu_lykong@126.com.

Abbreviations: ABC: ATP-binding cassette; BSA: Bovine serum albumin; DOX: Doxorubicin; FACS: Flow cytometry analysis; FBS: Fetal bovine serum; FITC: Fluorescein isothiocyanate; FS: *Fructus schisandra*; hMDR1-Luc: Human MDR1 luciferase reporter plasmid; LSCM: Laser scanning confocal microscopy; MDR: Multidrug resistance; MDR1: Multidrug resistance protein 1; MEM: Minimum essential medium; MG-63/DOX: Doxorubicin-resistant MG-63 subline; NF- κ B: Nuclear factor kappa-B; NF- κ B-Luc: NF- κ B luciferase reporter plasmid; P-gp: P-glycoprotein; PARP: Poly (ADP-ribose) polymerase; PDTC: Pyrrolidinedithiocarbamate; PI: Propidium iodide; RF: Reversal fold; Rh123: Rhodamine 123; RI: Resistance index; SchA: Schisandrin A; TNF- α : Tumor necrosis factor α ; Ver: Verapamil.

Grant sponsor: National Nature Science Foundation of China; Grant number: 81202901; Grant sponsor: Priority Academic Program Development of Jiangsu Higher Education Institutions (PAPD) and the Program for Changjiang Scholars and Innovative Research Team in University; Grant number: PCSIRT-IRT1193.

Abstract

The emergence of multidrug resistance (MDR) is a significant challenge in osteosarcoma chemotherapy. The central element of the MDR phenomenon is P-glycoprotein (P-gp, also called MDR1), an efflux transporter. Schisandrin A (SchA) extracted from *Fructus schisandra* has been reported to potently reverse MDR. However, the effect of SchA on osteosarcoma and the mechanism through which it inhibits MDR capacity remain unclear. In this study, SchA was tested for its potential to modulate the MDR phenotype and the function of P-gp in MG-63 doxorubicin-resistant (MG-63/DOX) cells. SchA increased the accumulation and retention of intracellular doxorubicin (DOX) in MG-63/DOX cells. Furthermore, it increased the accumulation of rhodamine 123 and decreased its efflux, indicating that SchA blocked P-gp. Furthermore, SchA enhanced DOX-induced apoptosis, reduced the expression of P-gp, and inhibited *MDR1* transcription. P-gp overexpression in MG-63 cells resulted in an increase in the IC_{50} value in response to DOX. Knockdown of P-gp in MG-63/DOX cells resulted in a decrease in IC_{50} value in response to DOX. Furthermore, P-gp overexpression in MG-63 cells or knockdown in MG-63/DOX cells resulted in changes in both cleaved-PARP and cleaved-caspase-7 levels in response to DOX. SchA reduced the IC_{50} of DOX and increased cleaved-PARP and cleaved-Caspase-7 levels in MG-63 cells transfected

with the *MDR1* expression vector. In addition, SchA inhibited NF- κ B signaling, TNF- α -induced p-I κ B- α and P-gp levels, and the TNF- α -induced increase in the IC₅₀ values of DOX. Taken together, these results support the potential therapeutic value of SchA as an MDR-reversing agent in chemotherapy for osteosarcoma.

Keywords: Schisandrin A; Multidrug resistance; Osteosarcoma; Doxorubicin; Nuclear Factor-kappa B

Introduction

Osteosarcoma, the most common primary malignant tumor of the bones in children and young adults, develops from mesenchymal cells and is pathologically characterized by spindle cells and aberrant osteoid formation. The incidence of osteosarcoma has a bimodal distribution with a peak in adolescence and a second peak occurring in the seventh and eighth decade of life.^{1,2} High-grade osteosarcoma can occur in any bone. Most commonly, osteosarcoma originates juxtaposed to the knee joint, and involves the distal femur (43%) or proximal tibia (23%). The proximal humerus, the next most common site of disease, is affected in approximately 10% of cases.³

Chemotherapy for osteosarcoma is often hampered by the rapid emergence of drug resistance, which exists for both conventional

chemotherapies and new drugs targeted to mutated or deregulated tumor cells.⁴ Diverse mechanisms are associated with the development of multidrug resistance (MDR), among which the most common is the overexpression of cell membrane-bound ATP-binding cassette (ABC) transporters.⁵⁻⁷ These proteins share the ability to transport a large number of structurally diverse and mainly hydrophobic compounds out of cells.⁸ The overexpression of P-glycoprotein (P-gp, MDR1 or ABCB1) is vital to the resistance of tumor cells against most chemotherapeutic regimens. P-gp has broad substrate specificity and is capable of transporting vinca alkaloids, anthracyclines, epipodophyllotoxins, and taxanes out of cells, as well as a wide range of other substances.⁹ A number of P-gp inhibitors and modulators have been described. Although many of these agents have been found to overcome drug resistance *in vitro*, *in vivo* results have been disappointing,^{2,10,11} primarily because of low host tolerance to experimental MDR modulators that precludes the attainment of active intracellular levels.^{12,13} In addition, these drugs may also expose the patients to undesired effects or alter the pharmacokinetics of co-administered anticancer drugs.¹⁴ These limitations have spurred efforts to search for new compounds with stronger effects against MDR and fewer side effects.

The plant known as *Fructus schisandra* (FS) in the Chinese Pharmacopoeia, and more commonly known as *Schisandra chinensis* or

the five flavor berry, has been applied as a medicinal herb in China for several millennia without reports of side effects, and is indexed as tonic and sedative.¹⁵ The 5 schizandrins that have been isolated from crude FS extract showed multiple biological activities, such as hepatoprotection (against cirrhosis or fibrosis), anti-oxidant activity, and inhibition of xenobiotic metabolism and mutagenicity.¹⁶ Among the schizandrins, schisandrin A (SchA) showed the most potent MDR reversal activity *in vitro* and *in vivo*.¹⁷ Another recent study reported that SchA affected the expression of membrane P-gp and inhibited P-gp efflux capability in the KB human epidermal carcinoma cell line and its vincristine-resistant variant cell line (KBv200).¹⁶ In addition, SchA also inhibited the expression of PKC and its translocation from the cytosol to membranes in MDR tumor cells.¹⁵ However, the ability of SchA to reverse drug resistance in osteosarcoma is unknown, and the molecular mechanisms through which it reverses MDR are not well understood.

In this study, we used a doxorubicin (DOX)-induced drug-resistant human osteosarcoma cell line, to evaluate the ability of SchA to enhance intracellular DOX accumulation and retention and DOX-induced apoptosis. Furthermore, we measured the effects of SchA on *MDR1* mRNA and protein expression. Finally, we investigated the involvement of nuclear factor kappa-B (NF- κ B) signaling in P-gp regulation.

Materials and methods

Materials

DOX, methotrexate, bleomycin, and vincristine were purchased from Santa Cruz Biotechnology (Santa Cruz, CA). Cisplatin, docetaxel, SchA (Fig. 1), verapamil (Ver), ammonium pyrrolidinedithiocarbamate (PDTC), MTT, rhodamine 123 (Rh123), RNase A, sodium pyruvate, paraformaldehyde, bovine serum albumin (BSA), Tris, NaCl, EDTA, NP-40, PMSF, NaF, SDS, and DTT were purchased from Sigma-Aldrich (St. Louis, MO). TNF- α was purchased from Peprotech (Rocky Hill, NJ). Opti-MEM and fetal bovine serum (FBS) were purchased from Life Technologies (Grand Island, NY). The fluorescein isothiocyanate (FITC)-conjugated mouse anti-human monoclonal antibody against P-gp and the corresponding isotype control were purchased from eBioscience (San Diego, CA). The annexin V-FITC/propidium iodide (AV-FITC/PI) apoptosis detection kit was purchased from BD Biosciences (San Diego, CA). The human MDR1 Luciferase reporter plasmid (hMDR1-Luc) was purchased from Takara (Dalian, China). The NF- κ B luciferase reporter plasmid (NF- κ B-Luc) was purchased from Beyotime (Haimen, China). The PRL-SV40 plasmid was purchased from Promega (Madison, WI). The P65-GFP plasmid was purchased from Addgene (Cambridge, MA).¹⁸ The *MDR1* plasmid was purchased from Genscript (Nanjing, China). The proteasome inhibitor MG-132 and the primary antibodies for p65, I κ B- α ,

p-I κ B- α (Ser32), cleaved-Caspase-7, cleaved-poly (ADP-ribose) polymerase (PARP), and PARP were purchased from Cell Signaling Technology (Danvers, MA). P-gp antibodies were purchased from Abcam Inc., (Cambridge, MA). GAPDH and lamin A antibodies were purchased from Sigma-Aldrich (St. Louis, MO). Rabbit anti-goat, goat anti-rabbit, and goat anti-mouse IgG-HRP-conjugated antibodies (Jackson Laboratories, West Grove, PA) were used as secondary antibodies.

Cell lines and cell culture

The human osteosarcoma cell line MG-63 was purchased from the Typical Culture Preservation Commission Cell Bank (Shanghai, China), and the MG-63 DOX-resistant subline (MG-63/DOX) was established and maintained in our laboratory. MG-63 and MG-3/DOX cells were cultured in MEM supplemented with 10% heat-inactivated FBS, 1.5 g/L NaHCO₃, and 0.11 g/L sodium pyruvate. Both cell types were incubated at 37 °C in a humidified atmosphere containing 5% CO₂.

Establishment of the DOX-resistant MG-63 subline

A DOX-resistant subline, MG-63/DOX, was established by gradually increasing the concentration of DOX to which the cells were exposed in a stepwise manner.¹⁹ The initial concentration (5 nM) of DOX added to the MG-63 cells was 0.05% of the concentration required to inhibit growth

by 50% (IC₅₀). The cultures were observed daily and allowed to grow, and underwent subsequent passages with the concentrations of DOX gradually increasing. The passaging was repeated for 8 months, after which the cells displayed 41.30-fold resistance to DOX compared with the corresponding parental sensitive cells. MG-63/DOX cells were maintained in culture medium containing 100 nM DOX and incubated in drug-free medium for at least 1 week before use.²⁰ All experiments were performed with cells in the logarithmic growth phase.

MTT assay

The MTT cytotoxicity assay was performed as described previously.²¹ Briefly, MG-63/DOX or MG-63 cells were seeded into 96-well culture plates at 4.5×10^3 cells/well. For the resistance index assay, serial dilutions of conventional chemotherapeutic drugs were added to the wells. For the MDR reversal activity assay, a full range of concentrations of conventional chemotherapeutic drugs with or without 10–50 μ M SchA or 10 μ M Ver (positive control) were added to the cells. After 48 h, 20 μ L of MTT solution (5 mg/mL in PBS) was added to each well, and the plates were incubated for an additional 4 h in a 37 °C incubator containing 5% CO₂, during which viable cells reduced yellow MTT into dark-blue formazan crystals. After incubation, 150 μ L of DMSO was added to each well and the plates were agitated for 10 min to dissolve the formazan

crystals. The absorbance in each well was read at 570 nm with background subtraction at 630 nm using a Molecular Devices SpectraMax Plus 384 microplate reader (Molecular Devices, Sunnyvale, CA, USA). IC_{50} values were calculated from survival curves using the Bliss method.²² The resistance index (RI) was calculated using the following formula:^{20,23} resistance index (RI) = IC_{50} (MG-63/DOX cells)/ IC_{50} (MG-63 cells). The reversal fold change, in terms of potency of reversal, was calculated using the following formula:^{5,24} reversal fold change (RF) = IC_{50} (MG-63/DOX cells)/ IC_{50} (MG-63/DOX cells combined with SchA treatment).

To measure the cell growth curve, MG-63 or MG-63/DOX cells were seeded into 96-well culture plates and incubated for 1–7 days, and MTT assay was performed. The average optical density was measured each day and used to plot the growth curve. For the cell viability assay, MG-63 or MG-63/DOX cells were incubated with 5–150 μ M SchA for 48 h, followed by the MTT assay. The percentage of cell survival was calculated by the following formula:²⁵ cell survival (%) = (mean absorbance in test wells)/(mean absorbance in control wells) \times 100.

To measure the inhibitory effect of SchA on P-gp, MG-63 cells were transfected with the *MDR1* plasmid or a mock plasmid, and MG-63/DOX cells were transfected with siMDR1 or siCon for 48 h and then incubated with serial dilutions of DOX in the absence or presence of SchA for

another 48 h, follow by the MTT assay.

To measure the inhibitory effect of SchA on NF- κ B signaling, MG-63 or MG-63/DOX cells were treated with serial dilutions of DOX with or without 20 μ M PDTC or 50 μ M SchA and/or 5 nM TNF- α for 48 h, followed by the MTT assay.

Intracellular accumulation and retention of DOX assay

The DOX accumulation and retention analyses were performed by laser scanning confocal microscopy (LSCM), as previously described.²⁴ In the accumulation assay, the MG-63/DOX cells were left to adhere for at least 12 h to poly (D-lysine)-coated glass coverslips, which were incubated for 24 h in medium containing DOX (5 μ M) with or without SchA (50 μ M) or Ver (10 μ M). In the retention experiment, the MG-63/DOX cells were incubated for 24 h in a medium containing DOX (5 μ M), and then washed 3 times with warm culture medium. The cells were incubated for 24 h in a medium with or without SchA (50 μ M) or Ver (10 μ M). Subsequently, the culture medium was removed and cells were washed 3 times with PBS. Cells were fixed in 4% paraformaldehyde for 10 min at 25 °C, washed 3 times with PBS, and the fluorescence intensity of intracellular DOX was measured. Fluorescence was excited at 465–495 nm and detected at an emission maximum of 515–555 nm. Intracellular DOX was quantified using Image Pro Plus 6.0 (Media Cybernetics, Inc.,

Rockville, MD, USA).

Detection of the effects of SchA on the function and expression of P-gp using flow cytometry

The function of P-gp was assessed by measuring the intracellular accumulation and efflux of Rh123 as previously described.²⁴ In the accumulation analysis, MG-63 and MG-63/DOX cells were pretreated with or without 50 μM SchA or 10 μM Ver for 1 h and then incubated with 5 μM Rh123 in the dark for 1 h. In the efflux study, MG-63 and MG-63/DOX cells were first cultured with medium containing 5 μM Rh123 at 37 °C for 1.5 h, washed 3 times with PBS, then incubated in the absence or presence of 50 μM SchA at 37 °C for another 1.5 h (or with 10 μM Ver as a positive control). After incubation, all cells were washed twice with ice-cold PBS and subjected to flow cytometric analysis (FACS) to detect green fluorescence produced by Rh123.

The expression of cell surface P-gp was analyzed by flow cytometry. MG-63 or MG-63/DOX cells were pretreated with or without 50 μM SchA for 24–48 h, and then they were harvested, washed twice with PBS, and labeled with FITC-conjugated mouse anti-human monoclonal antibody against P-gp or a control isotype according to the manufacturer's instructions.

Apoptosis assay

Apoptosis was determined by flow cytometry in accordance with the manufacturer's instructions. An AV-FITC/PI double-staining assay was used to analyze apoptosis induced by SchA, for which MG-63 or MG-63/DOX cells were incubated with 0–150 μM SchA for 48 h. In addition, an AV-FITC/PI double-staining assay was used to analyze apoptosis induced by DOX, for which MG-63/DOX cells were maintained in medium containing DOX (1 μM) with or without SchA (50 μM) or Ver (10 μM) for 48 h. Cells were washed twice with cold PBS, suspended in 500 μL of binding buffer at a concentration of 1×10^6 cells/mL, and annexin V and PI (5 μL) were added. The cells were gently vortexed and incubated for 15 min at 25 $^{\circ}\text{C}$ in the dark, after which fluorescence was immediately determined by flow cytometry. Statistical analysis was performed using FlowJo software (Tree Star Inc., Ashland, OR, USA). The percentage of early apoptotic cells was calculated by the dimension of annexin V positive, but PI negative, while the percentage late apoptotic and necrotic cells was calculated by the dimension of annexin V positive and PI positive.

Plasmid transfection and luciferase reporter assay

Plasmid preparation was performed and as previously described with some modifications.²⁶ A dual-luciferase reporter assay system was used to

determine the activities of the MDR1 and NF- κ B promoters. MG-63 or MG-63/DOX cells were co-transfected transiently with an hMDR1-Luc or NF- κ B-Luc reporter plasmid and the *Renilla* luciferase reporter, and pRL-SV40 plasmid as an internal control. Cells were transfected using Opti-MEM containing 10 μ g of plasmids and the Super Electroporator NEPA21 system (NEPAGENE, Japan). Thirty-six h after transfection, cells were treated with 0–50 μ M SchA for 8 h with 1 μ M DOX and/or 50 μ M SchA for 8 h, or for 8 h with 1 μ M DOX and/or 50 μ M SchA and for 4 h with 5 nM TNF- α . Luciferase activity in cell lysates was measured using a luminometer (TD-20; Turner Designs, Sunnyvale, CA). Relative luciferase activity was calculated by normalizing MDR1 or NF- κ B promoter-driven firefly luciferase activity to *Renilla* luciferase activity (Luminoskan Ascent, Thermo Electron).

In addition, MG-63 cells were transfected transiently with 10 μ g of p65-GFP plasmid, and after 48 h were treated with 0–50 μ M SchA for 48 h prior to harvesting.

Overexpression of P-gp in MG-63 cells and deregulation of P-gp in MG-63/DOX cells

MG-63 cells were transfected with the *MDR1* plasmid or a mock plasmid for 48 h, and treated with or without 1 μ M DOX in the absence or presence of 50 μ M SchA for 48 h, followed by Western blot analysis.

The siRNA sequences used for transient transfections were previously described:²⁷ siMDR1 is 5'-GGAAAAGAAACCAACUGUCdTdT-3' and siCon is 5'-UUCUCCGAACGUGUCACGUCdTdT-3'. Transfection was performed using the Super Electroporator NEPA21 system. Briefly, 1×10^6 MG-63/DOX cells were transfected using Opti-MEM containing 150 pM siRNA oligos. Forty-eight h later, cells were treated with or without 1 μ M DOX in the absence or presence of 50 μ M SchA for 48 h, followed by Western blot analysis.

Quantitative real-time RT-PCR

The quantitative real-time polymerase chain reaction (qRT-PCR) was performed as previously described.²⁸ The Δ cycle threshold method was used for the calculation of relative differences in mRNA abundance with a LightCycler 480 (Roche Molecular Biochemicals, Mannheim, Germany). Data were normalized to the expression of *GAPDH*. The results of real-time RT-PCR were expressed as fold-changes. The normalized value of the target mRNA of the control group is arbitrarily presented as 1. The sequences of primers used were as follows: *MDR1*, 5'-AGAGTCAAGGAGCATGGCAC-3' (sense) and 5'-ACAGTCAGAGTTCCTGGCG-3' (antisense); and *GAPDH*, 5'-GAAAGCCTGCCGGTGACTAA-3' (sense) and 5'-AGGAAAAGCATCACCCGGAG-3' (antisense).

Western blot analysis

Protein levels were determined by standard Western blot. Briefly, after treatment MG-63 or MG-63/DOX cells were washed twice with PBS, collected, and lysed in lysis buffer (100 mM Tris-HCl, pH 6.8, 4% w/v SDS, 20% v/v glycerol, 200 mM β -mercaptoethanol, 1 mM phenylmethylsulfonyl fluoride, and 1 g/mL aprotinin). Lysates were centrifuged at 12000 g for 30 min at 4 °C. Protein was extracted using the Membrane Protein Extraction Kit, Total Protein Extraction Kit, or Nuclear and Cytoplasmic Protein Extraction Kit (Beyotime, Haimen, Jiangsu, China) according to the manufacturer's instructions. The protein concentration was determined using the BCA assay with a Molecular Devices SpectraMax Plus 384 microplate reader (Molecular Devices, Sunnyvale, CA, USA) at 562 nm. Next, 38 μ g (total) or 20 μ g (membrane, nuclear or cytoplasmic) of protein samples were separated with 10% or 8% SDS-PAGE and transferred onto PVDF membranes (Bio-Rad Inc., Hercules, CA, USA). Immune complexes were formed by the incubation of proteins with primary antibodies (1:1000 dilution) overnight at 4 °C, followed by secondary antibodies (1:10000 dilution) for 2 h at 25 °C. After extensive washing with TBST, membranes were process with the EasySee Western Blot Kit (TransGen Biotech, Beijing, China) according to the manufacturer's protocol. Immunoreactive protein bands were

detected with a ChemiDOC XRS+ (Bio-Rad, Inc.). Image Lab 4.0 (Bio-Rad, Inc., Hercules, CA) was used to quantify protein expression based on band intensity.

Statistical analysis

All quantitative results were reported as mean \pm S.D. of the data from at least three experiments performed in a parallel manner. Statistical analysis was performed with the GraphPad Prism 5 software.

Results

MG-63/DOX cells show high resistance to DOX and display MDR to other conventional chemotherapeutic drugs

The cell growth curve showed that MG-63/DOX cells had a logarithmic phase that was similar to that of MG-63 cells. However, MG-63 cells grew faster than MG-63/DOX cells and there were significant differences in growth between MG-63 and MG-63/DOX cells on days 3, 4, and 5 (Fig. 2A). Next, we determined the resistance index of MG-63/DOX cells in comparison with their parental sensitive MG-63 cells. The IC₅₀ values of MG-63/DOX and MG-63 cells for DOX were 48.32 ± 2.52 and 1.17 ± 0.50 μ M, respectively. The RI value was 41.30 (Fig. 2A), indicating that the resistant subline exhibited high resistance (RI > 20) to DOX.²³ Table 1 shows the MG-63/DOX cell MDR data for other chemotherapeutic drugs.

These results showed that the MG-63 DOX-resistant subline was successfully established.

SchA has potent anti-MDR activity in MG-63/DOX cells

We tested whether SchA had anti-MDR activity in MG-63/DOX cells. The IC₅₀ values of DOX, DOX plus 10 μ M Ver, and DOX plus 10–50 μ M SchA in MG-63/DOX cells were 8.54 ± 1.37 , and 5.70 ± 1.10 , and 4.57 ± 1.50 and 3.26 ± 0.70 μ M, respectively. The reversal fold change of SchA was 8.48–15.1, and that of Ver was 5.66 (Fig. 2B). SchA also enhanced the sensitivity of MG-63/DOX cells to other conventional chemotherapeutic drugs (Table 1).

SchA enhances DOX-induced apoptosis of MG-63/DOX cells by increasing intracellular DOX accumulation

In order to identify the concentration at which SchA is nontoxic to cells, but enhances DOX-induced apoptosis, we assayed the cytotoxicity of SchA at concentrations ranging from 0 to 150 μ M. SchA at concentrations lower than 50 μ M did not significantly inhibit the growth of MG-63 or MG-63/DOX cells, as measured by the MTT assay (inhibition < 10%) (Fig. 3A), and also did not significantly increase the number of apoptotic cells (early and late apoptotic cells < 10%) as assayed by AV-FITC/PI analysis (Fig. 3B). More than 90% viable cells were detected after

treatment with 50 μM SchA. Therefore, unless otherwise stated, SchA at 50 μM was used for the subsequent studies.

To test whether SchA enhances DOX-induced apoptosis, we performed AV-FITC/PI analysis. We observed a notable increase in early and late phase apoptosis when cells were treated with DOX and SchA together (early phase apoptosis percentages: DOX, $10.27 \pm 2.30\%$; DOX combined with Ver, $23.70 \pm 2.78\%$; and DOX combined with SchA, $31.13 \pm 3.65\%$; late phase apoptosis percentages: DOX, $3.10 \pm 1.40\%$; DOX combined with Ver, $21.70 \pm 1.78\%$; and DOX combined with SchA: $44.50 \pm 5.17\%$) (Fig. 3C). Thus, SchA showed low toxicity in MG-63 or MG-63/DOX cells at 50 μM when administered alone, but enhanced the cytotoxicity of DOX in MG-63/DOX cells.

In addition, cleavage of Caspase-7 and PARP served as indicators of the activation and onset of apoptosis. We speculate that SchA promotes Caspase-7 and PARP activation and increases cleavage of Caspase-7 and PARP. Not surprisingly, treatment with SchA increased levels of cleaved Caspase-7 and PARP compared to the other groups (Fig. 3D).

We then investigated the manner in which SchA enhanced DOX-induced cell death by FACS and LSCM. We speculated that P-gp may play an important role in DOX efflux. Therefore, we investigated the effect of SchA on P-gp function by detecting the accumulation and efflux of P-gp-specific substrate Rh123.²⁴ Rh123 uptake occurs via passive

inward diffusion, while its efflux is P-gp dependent. As a result, Rh123 has been used extensively as an indicator of P-gp activity. FACS analysis indicated that MG-63/DOX cells contained much less Rh123 than did MG-63 cells. The accumulation of Rh123 in MG-63/DOX cells treated with SchA was higher than that in positive control (Ver) cells (Rh123 fluorescence intensity: 825.5 ± 22.81 , 882.1 ± 18.85 , and 1052 ± 86.23 for Rh123, Rh123 combined with Ver, and Rh123 combined with SchA, respectively). In the Rh123 efflux experiment, a rapid decrease in intracellular Rh123 content was observed in MG-63/DOX cells after incubation in Rh123-free medium for 1.5 h. Treatment of MG-63/DOX cells with SchA suppressed Rh123 efflux, suggesting its inhibitory effect on P-gp-mediated active transport (Rh123 fluorescence intensity: 558.5 ± 13.87 , 700.5 ± 87.11 , and 971.5 ± 136.7 for Rh123, Rh123 combined with Ver, and Rh123 combined with SchA, respectively). Neither Ver nor SchA showed any significant effect on Rh123 accumulation and efflux in MG-63 cells (Rh123 fluorescence intensity: accumulation: 1565 ± 181.1 , 1633 ± 194.9 , and 1755 ± 239.6 ; efflux: 1135 ± 180.9 , 1177 ± 228.5 , and 1350 ± 381.9 for Rh123, Rh123 combined with Ver, and Rh123 combined with SchA, respectively) (Fig. 3E).

DOX is a substrate of P-gp.²⁹ We measured the accumulation and retention of DOX in MG-63/DOX cells to confirm the role of SchA in the inhibitory effect on P-gp activity. In intracellular DOX accumulation and

effusion assays, LSCM analysis showed that, compared with DOX alone or DOX combined with Ver, SchA significantly increased intracellular DOX accumulation (light intensity: 12.66 ± 0.63 , 16.58 ± 2.09 , and 22.31 ± 1.05 for DOX alone, DOX combined with Ver, and DOX combined with SchA, respectively) and decreased DOX effusion (light intensity: 7.34 ± 0.36 , 9.95 ± 0.54 , and 11.04 ± 1.21 for DOX alone, DOX combined with Ver, and DOX combined with SchA, respectively) (Fig. 3F). These results showed that SchA enhanced the cytotoxicity of DOX by increasing intracellular concentrations of DOX and reduced the efflux of DOX by inhibiting P-gp function in MG-63/DOX cells.

SchA reverses MDR by inhibiting P-gp expression in MG-63/DOX cells

We found that the *MDR1* mRNA level of MG-63/DOX cells was significantly higher than that of MG-63 cells. SchA inhibited *MDR1* expression in a time-dependent manner (Fig. 4A). P-gp levels at the membrane surface were detected by FACS (Fig. 4B), and Western blot analysis (Fig. 4C) confirmed these results. In addition, SchA had little effect on P-gp expression in MG-63 cells, but SchA inhibited *MDR1* transcription in a concentration-dependent manner (Fig. 4D). Thus, the inhibitory effect of SchA on the expression of P-gp would be expected to increase DOX retention in MG-63/DOX cells.

In order to determine the role of P-gp in the effect of SchA on MDR, we transfected MG-63 cells with the *MDR1* expression vector and treated MG-63/DOX cells with *MDR1* siRNA. After transfection, SchA reduced P-gp expression (Fig. 4E) and increased the cytotoxicity of DOX (Fig. 4F) in MG-63 cells (IC_{50} of DOX: $1.89 \pm 1.41 \mu\text{M}$). The MTT assay indicated that overexpression of P-gp in MG-63 cells increased the IC_{50} value of DOX ($12.97 \pm 5.03 \mu\text{M}$) and down-regulation of P-gp in MG-63/DOX cells decreased the IC_{50} value of DOX ($22.91 \pm 2.18 \mu\text{M}$). Furthermore, MG-63/DOX cells with P-gp knockdown were treated with SchA and examined using the MTT assay, and the IC_{50} value of DOX ($2.76 \pm 1.28 \mu\text{M}$) was found to be significantly reduced (Fig. 4F). In addition, up-regulation of P-gp by *MDR1* plasmid in MG-63 cells or reduction of P-gp by siRNA in MG-63/DOX cells did not result in detectable changes in levels of the apoptotic markers PARP and Caspase-7 prior to DOX treatment, demonstrating that under normal growth conditions, P-gp overexpression or reduction of P-gp levels had little effect upon apoptotic pathway activation (Fig. 4G). In response to DOX treatment, overexpression of P-gp in MG-63 cells led to a decreased level of cleaved PARP. Treatment with SchA reversed this decrease. Loss of P-gp expression in MG-63/DOX cells led to a more rapid onset and increased level of cleaved PARP. SchA further increased the level of cleaved PARP after treatment with *MDR1* siRNA in MG-63/DOX cells. Examination of

cleaved-Caspase-7 in MG-63 and MG-63/DOX cells showed a similar trend to that of PARP cleavage (Fig. 4G). Taken together, these data demonstrate that P-gp expression promotes cell survival in MG-63 and MG-63/DOX cells in response to DOX, and SchA reverses MDR by inhibiting P-gp expression.

SchA inhibits NF- κ B signaling in an IKK-dependent manner in MG-63/DOX cells

NF- κ B activation regulates *MDR1* gene expression.³⁰ We investigated whether NF- κ B signaling was activated in MG-63/DOX cells, and whether any observed inhibitory effect of SchA led to NF- κ B signaling down-regulation. Western blot experiments indicated that p65 protein levels in MG-63/DOX cells were dramatically higher than those in MG-63 cells, and that SchA inhibited p65 translocation to the nucleus and increased p65 protein abundance in the cytoplasm. Total p65 levels appeared constant in MG-63/DOX cells (Fig. 5A).

To further determine the effect of SchA on NF- κ B signaling, MG-63/DOX cells were treated with SchA, and I κ B- α and p-I κ B- α protein levels were detected. Western blot results demonstrated that SchA inhibited I κ B- α phosphorylation and degradation in a concentration-dependent manner (Fig. 5B). In addition, dual-luciferase reporter experiments indicated that SchA inhibited NF- κ B activity in a

concentration-dependent manner (Fig. 5C). Thus, SchA suppresses NF- κ B signaling in an IKK-dependent manner in MG-63/DOX cells.

SchA reduces P-gp by inhibiting NF- κ B signaling

TNF- α is an NF- κ B signaling stimulator that activates NF- κ B, promotes I κ B- α phosphorylation, and increases P-gp expression.^{31,32} PDTC is a specific NF- κ B inhibitor that reduces P-gp expression.³⁰ We used the MTT assay to evaluate changes induced by TNF- α and PDTC. In MG-63 cells, the results indicated that after incubation with TNF- α , DOX resistance (IC₅₀ of DOX: 9.73 \pm 4.52 μ M) was induced, whereas SchA inhibited TNF- α -induced DOX resistance (IC₅₀ of DOX: 2.26 \pm 1.83 μ M). Similar results were observed in MG-63/DOX cells, in which incubation with TNF- α further increased the IC₅₀ value of DOX (57.85 \pm 6.46 μ M), but the TNF- α -induced DOX resistance was reversed by treatment with SchA (IC₅₀ of DOX: 7.15 \pm 3.73 μ M). Treatment with PDTC also significantly decreased the IC₅₀ value of DOX (16.31 \pm 1.35 μ M) (Fig. 6A).

Western blot experiments confirmed that TNF- α promoted I κ B- α phosphorylation, which was inhibited by SchA in MG-63 cells. In MG-63/DOX cells, SchA enhanced the inhibitory effect of PDTC on I κ B- α phosphorylation (Fig. 6B). Furthermore, TNF- α increased expression of P-gp in MG-63 and MG-63/DOX cells, and SchA

decreased these stimulatory effects. In addition, SchA enhanced the inhibitory effect of PDTC on P-gp expression in MG-63/DOX cells (Fig. 6C). To further evaluate the involvement of NF- κ B in the suppression of P-gp expression by SchA, MG-63 cells were transfected with a p65-GFP plasmid. As expected, p65-GFP enhanced P-gp expression, and this effect was inhibited by SchA in a concentration-dependent manner (Fig. 6D).

SchA reduces DOX-induced I κ B- α phosphorylation and enhances the inhibitory effect of DOX on NF- κ B transcriptional activity

It is interesting that DOX has the ability to inhibit NF- κ B-dependent gene expression while inducing I κ B- α phosphorylation;³³ therefore, we determined the effect of DOX with or without SchA on NF- κ B transcriptional activity in our MDR model. Luciferase reporter experiments (Fig. 7A) indicated that DOX significantly repressed NF- κ B transcriptional activity in MG-63 cells. SchA produced a weaker inhibitory effect than DOX, but the combination of SchA and DOX produced a stronger inhibitory effect than SchA. In MG-63/DOX cells, the inhibitory effect of DOX on the NF- κ B reporter plasmid was weaker than that observed in MG-63 cells, but SchA showed a stronger inhibitory effect on NF- κ B transcriptional activity. When combined with SchA, DOX recovered its inhibitory effect.

We were interested in the mechanisms of I κ B- α activation by DOX and

whether or not SchA had a similar effect on I κ B- α in MG-63 and MG-63/DOX cells. In MG-63 cells (Fig. 7B), we found that exposure to DOX was accompanied by I κ B- α degradation, while there was no significant change after exposure to SchA. Moreover, incubation with the proteasome inhibitor MG-132 revealed inducible I κ B- α phosphorylation at serine 32 by DOX. SchA showed little effect on I κ B- α phosphorylation, but significantly inhibited I κ B- α phosphorylation induced by DOX. A different situation was found in MG-63/DOX cells (Fig. 7B). DOX had a slight enhancing effect on I κ B- α phosphorylation and degradation. We deduced that DOX was not retained at sufficient levels in MG-63/DOX cells to produce stronger effects. Treatment with SchA significantly inhibited I κ B- α phosphorylation and degradation. In addition, its inhibition of I κ B- α decreased the activating effect of DOX on I κ B- α .

To further verify the IKK-dependent mechanism of SchA, we used TNF- α to activate NF- κ B and I κ B- α . In MG-63 cells (Fig. 7C), treatment with TNF- α strongly enhanced the activity of the transfected NF- κ B luciferase reporter plasmid. DOX and SchA significantly decreased subsequent TNF- α -induced NF- κ B transcriptional activity. Not surprisingly, in MG-63/DOX cells (Fig. 7C), SchA enhanced the inhibitory effect of DOX. Furthermore, DOX enhanced TNF- α -induced I κ B- α phosphorylation in MG-63 cells, but did not significantly affect TNF- α -induced I κ B- α phosphorylation in MG-63/DOX cells. In addition,

SchA inhibited TNF- α - and DOX-induced I κ B- α phosphorylation, especially in MG-63/DOX cells (Fig. 7D).

We confirm the activating effect of DOX on I κ B- α phosphorylation and the inhibitory effect of DOX on NF- κ B transcriptional activity. If this is the case, P-gp, which is regulated by NF- κ B³⁰ should be inhibited by DOX. However, in the DOX-induced MG-63 resistant subline, P-gp levels and NF- κ B signaling were up-regulated (Fig. 4C and Fig. 5A). Thus, we analyzed the effect of DOX on *MDR1* mRNA levels at each time point in MG-63 cells. QRT-PCR results indicated that DOX decreased *MDR1* mRNA levels at 12 h, but induced *MDR1* mRNA expression after 12 h in a time-dependent manner. In addition, SchA significantly inhibited DOX-induced changes in *MDR1* mRNA levels (Fig. 7E).

Discussion

We found that NF- κ B signaling was significantly activated in MG-63/DOX cells compared with MG-63 cells. Following DOX stimulation, the transcriptional activity of NF- κ B was repressed, but the phosphorylation of I κ B- α was promoted. We speculate that DOX activates I κ B- α phosphorylation to promote p65 translocation to nucleus and induces the conversion of nuclear p65 from an activator of gene expression to a repressor via the recruitment of corepressor complexes³³

to inhibit NF- κ B transcriptional activity. If this is the case, combined treatment of cells with TNF- α , which provides the stimuli necessary to induce p65 transactivation, and DOX should result in the inhibition of NF- κ B-dependent, TNF- α -induced NF- κ B transcriptional activity. We confirmed that the treatments shown in Fig. 7C resulted in inhibition of subsequent TNF- α -induced NF- κ B transcriptional activity. SchA repressed I κ B- α phosphorylation induced by DOX or TNF- α and inhibited NF- κ B transcriptional activity. Taken together with the results in Fig. 5A, this finding suggests that SchA suppresses NF- κ B activity by inhibiting p65 activation and translocation to the nucleus in MG-63/DOX cells.

It was interesting that SchA showed a small effect on NF- κ B activity in MG-63 cells, but exhibited potent inhibition of NF- κ B activity in MG-63/DOX cells. We deduced that SchA combined with IKK or I κ B- α to inhibit I κ B- α phosphorylation in the cytoplasm and cooperated with activated p65 to repress NF- κ B transcription in the nucleus. Treatment with TNF- α verified that SchA inhibited subsequent TNF- α -induced NF- κ B activity in MG-63 cells (Fig. 7C). This effect was also the reason that SchA combined with DOX did not significantly inhibit NF- κ B transcriptional activity compared with treatment with DOX alone in MG-63 cells (Fig. 7A). These results indicated that NF- κ B activation was inhibited by SchA through canonical pathways (based on impeditive

I κ B- α -degradation that prevents NF- κ B dimers (mainly p65/p50 dimers) from accumulating in the nucleus and activate transcription).^{34,35} In addition, SchA enhanced the cytotoxicity of DOX by increasing intracellular DOX accumulation in MG-63/DOX cells. As shown in Fig. 7D, phosphorylation of I κ B- α was detected without the proteasome inhibitor MG-132 in MG-63/DOX cells. We deduced that I κ B- α might be activated continuously in MG-63/DOX cells; this effect would activate NF- κ B signaling and further promote I κ B- α expression.

The high fold change of P-gp expression in MG-63 resistant subline was induced by DOX. SchA showed little effect on *MDR1* gene (Fig. 4A) and protein expression (Fig. 4B and C) in MG-63 cells but exhibited significant inhibition in MG-63/DOX cells. In *MDR1* mRNA level, SchA showed inhibitory effect at 12 h in MG-63/DOX cells which differs from the protein level. Besides, all inhibitions were happened effectively after 24 h but significantly at 48 h (Fig. 4A, B and C). Luciferase report experiments confirmed the inhibitory effect of SchA on *MDR1* transcription in MG-63/DOX cells (Fig. 4D). The inhibitory effect of SchA on overexpression of P-gp in transfected MG-63 cells also confirmed the results. In addition, Western blot results indicated that transfected with *MDR1* siRNA led to a sharp decrease of P-gp in MG-63/DOX cells (Fig. 4E), which was the main reason to resensitization of MG-63/DOX cells to DOX (Fig. 4F). These results also

demonstrated that P-gp plays an important role in drug resistance in MG-63 cells. Besides, after down-regulation of P-gp by siRNA in MG-63/DOX cells, treatment with SchA further enhanced DOX-induced cytotoxicity (Fig. 4F), indicating that other anti-MDR mechanism exists that are P-gp-independent. In addition, without treatment with DOX, changing P-gp expression produced little effect on levels of cleaved-PARP and cleaved-Caspase-7 in MG-63 and MG-63/DOX cells (Fig. 4G). These effects demonstrated that although SchA had the ability to inhibit P-gp function and expression; apoptosis and cytotoxicity were not induced by SchA (Fig. 3A, B and C), but by DOX.

SchA is the most abundant active dibenzocyclooctadiene derivative isolated from *Fructus schisandra*. However, to our knowledge, no existing evidence shows that SchA has anti-MDR activity in osteosarcoma. Our data demonstrated the powerful MDR reversal effect of SchA and illustrated the mechanisms of this anti-MDR activity in MG-63/DOX cells. In contrast, SchA had no apparent effect in the drug-sensitive MG-63 cell line (Fig. 3E; Fig. 4A, B, and C; and Fig. 7A and B). In addition, we found that SchA also had an anti-MDR effect in cisplatin-resistant MG-63 cells (data not shown).

Conclusion

Our findings demonstrate for the first time that SchA is able to reverse

P-gp-mediated DOX resistance in osteosarcoma cells by blocking P-gp and NF- κ B signaling. SchA reversed MDR in MG-63/DOX cells by promoting nuclear DOX accumulation. Because of its potent anti-MDR effect and low toxicity, SchA is a potential candidate adjuvant therapy for drug resistant cancers.

Conflict of Interest

The authors declare that there are no conflicts of interest.

References

- 1 L. Mirabello, R.J. Troisi and S.A. Savage, *Cancer*, 2009, **115**, 1531–1543.
- 2 J. Gill, M.K. Ahluwalia, D. Geller and R. Gorlick, *Pharmacol. Ther.*, 2013, **37**, 89–99.
- 3 S.S. Bielack, B. Kempf-Bielack, G. Delling, G.U. Exner, S. Flege, K. Helmke, R. Kotz, M. Salzer-Kuntschik, M. Werner, W. Winkelmann, A. Zoubek, H. Jürgens and K. Winkler, *J. Clin. Oncol.*, 2002, **20**, 776–790.
- 4 S. Huang, M. Hölzel, T. Knijnenburg, A. Schlicker, P. Roepman, U. McDermott, M. Garnett, W. Grernrum, C. Sun, A. Prahallad, F.H. Groenendijk, L. Mittempergher, W. Nijkamp, J. Neefjes, R. Salazar, P. Ten Dijke, H. Uramoto, F. Tanaka, R.L. Beijersbergen, L.F. Wessels

- and R. Bernards, *Cell*, 2012, **151**, 937–950.
- 5 X.Q. Zhao, J.D. Xie, X.G. Chen, H.M. Sim, X. Zhang, Y.J. Liang, S. Singh, T.T. Talele, Y. Sun, S.V. Ambudkar, Z.S. Chen and L.W. Fu, *Mol. Pharmacol.*, 2012, **82**, 47–58.
- 6 M. Dean, A. Rzhetsky and R. Allikmets, *Genome. Res.*, 2001, **11**, 1156–1166.
- 7 R. Pérez-Tomás, *Curr. Med. Chem.*, 2006, **13**, 1859–1876.
- 8 G. Szakács, J.K. Paterson, J.A. Ludwig, C. Booth-Genthe and M.M. Gottesman, *Nat. Rev. Drug Discov.*, 2006, **5**, 219–234.
- 9 S.V. Ambudkar, S. Dey, C.A. Hrycyna, M. Ramachandra, I. Pastan and M.M. Gottesman, *Annu. Rev. Pharmacol. Toxicol.*, 1999, **39**, 361–398.
- 10 T. Tsuruo, H. Iida, M. Nojiri, S. Tsukagoshi and Y. Sakurai, *Cancer Res.*, 1983, **43**, 2905–2910.
- 11 A. Kiue, T. Sano, A. Naito, M. Okumura, K. Kohno and M. Kuwano, *Br. J. Cancer*, 1991, **64**, 221–226.
- 12 F. Hyafil, C. Vergely, P. Du Vignaud and T. Grand-Perret, *Cancer Res.*, 1993, **53**, 4595–4602.
- 13 J.M. Ford and W.N. Hait, *Pharmacol. Rev.*, 1990, **42**, 155–199.
- 14 R. Krishna and L.D. Mayer, *Eur. J. Pharm. Sci.*, 2000, **11**, 265–283.
- 15 W.L. Li, H.W. Xin and M.W. Su, *Basic Clin. Pharmacol. Toxicol.*, 2011, **110**, 187–192.
- 16 M. Huang, J. Jin, H. Sun and G.T. Liu, *Cancer Chemother.*

- Pharmacol.*, 2008, **62**, 1015–1026.
- 17 S.J. Kim, H.Y. Min, E.J. Lee, Y.S. Kim, K. Bae, S.S. Kang and S.K. Lee, *Phytother. Res.*, 2010, **24**, 193-197.
- 18 Lf. Chen, W. Fischle, E. Verdin and W.C. Greene, *Science*, 2001, **293**, 1653-1657.
- 19 T. Yamauchi, Y. Matsuda, T. Tasaki, E. Negoro, S. Ikegaya, K. Takagi, A. Yoshida, Y. Urasaki and T. Ueda, *Cancer Sci.*, 2012, **103**, 1722–1729.
- 20 N. Wei, G.T. Liu, X.G. Chen, Q. Liu, F.P. Wang and H. Sun, *Biochem. Pharmacol.*, 2011, **82**, 1593–1603.
- 21 M.Z. El-Readi, S. Eid, M.L. Ashour, A. Tahrani and M. Wink, *Phytomedicine*, 2013, **20**, 282–294.
- 22 Z. Shi, Y.J. Liang, Z.S. Chen, X.W. Wang, X.H. Wang, Y. Ding, L.M. Chen, X.P. Yang and L.W. Fu, *Cancer Biol. Ther.*, 2006, **5**, 39–47.
- 23 K. Snow and W. Judd, *Br. J. Cancer*, 1991, **63**, 17–28.
- 24 L. Yang, D.D. Wei, Z. Chen, J.S. Wang and L.Y. Kong, *Phytomedicine*, 2011, **18**, 710–718.
- 25 L. Li, Q. Lu, Y. Shen and X. Hu, *Biochem. Pharmacol.*, 2006, **71**, 584–595.
- 26 L. Wang, Q. Meng, C. Wang, Q. Liu, J. Peng, X. Huo, H. Sun, X. Ma and K. Liu, *J. Nat. Prod.*, 2013, **76**, 909–914.
- 27 H. Wu, W.N. Hait and J.M. Yang, *Cancer Res.*, 2003, **63**, 1515-1519.

- 28 S.R. Kim, D.I. Kim, M.R. Kang, K.S. Lee, S.Y. Park, J.S. Jeong and Y.C. Lee, *J. Allergy Clin. Immunol.*, 2013, **132**, 1397-1408.
- 29 M.M. Gottesman, T. Fojo and S.E. Bates, *Nat. Rev. Cancer*, 2002, **2**, 48–58.
- 30 H.Y. Yang, L. Zhao, Z. Yang, Q. Zhao, L. Qiang, J. Ha, Z.Y. Li, Q.D. You and Q.L. Guo, *Mol. Carcinog.*, 2012, **51**, 185–195.
- 31 T.T. Hien, H.G. Kim, E.H. Han, K.W. Kang and H.G. Jeong, *Mol. Nutr. Food Res.*, 2010, **54**, 918–928.
- 32 L. Wang, C. Wang, J. Peng, Q. Liu, Q. Meng, H. Sun, X. Huo, P. Sun, X. Yang, Y. Zhen and K. Liu, *Toxicol. Appl. Pharmacol.*, 2014, **277**, 146-154.
- 33 K.J. Campbell, S. Rocha and N.D. Perkins, *Mol. Cell.*, 2004, **13**, 853-865.
- 34 S. Banerjee, A.K. Sahoo, A. Chattopadhyay and S.S. Ghosh, *RSC Adv.*, 2014, **4**, 39257-39267.
- 35 Z. Sun and R. Andersson, *Shock* , 2002, **18**, 99–106.

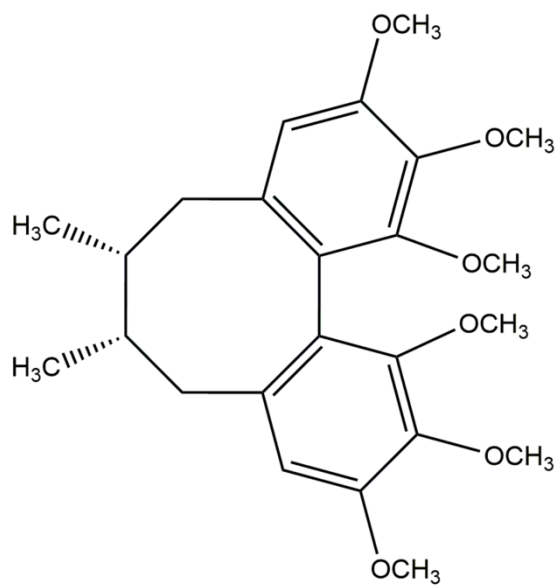
Table 1 The resistance indexes of MG-63/DOX cells and the reverse effects of SchA in the MG-63/DOX cells for other conventional chemotherapeutic drugs.

Drug	IC ₅₀ (μM)			RI ^a	RF ^b
	MG-63	MG-63/DOX			
		Vehicle	+ SchA		
Cisplatin	2.82±0.57	15.98±1.04	6.92±0.59	5.67	2.31
Docetaxel	0.79±0.12	5.74±0.74	2.32±0.52	7.26	2.47
Bleomycin	4.79±0.64	25.63±1.25	10.27±0.72	5.35	2.50
Vincristine	0.84±0.10	8.24±0.56	1.07±0.29	9.81	7.70
Methotrexate	0.71±0.03	5.85±0.47	2.06±0.58	8.24	2.84

The results were reported as mean ± S.D. of the data from at least three experiments performed in a parallel manner.

^aResistance index (RI) = IC₅₀ (MG-63/DOX cells)/IC₅₀ (MG-63 cells).

^bReversal fold change (RF) = IC₅₀ (MG-63/DOX cells)/IC₅₀ (MG-63/DOX cells combined with SchA treatment).



Schisandrin A Molecular Formula: C₂₄H₃₂O₆
Molecular Weight: 416.51

Fig. 1.

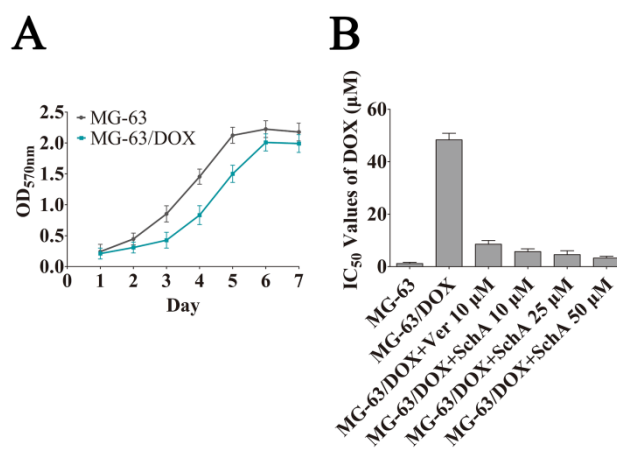


Fig. 2.

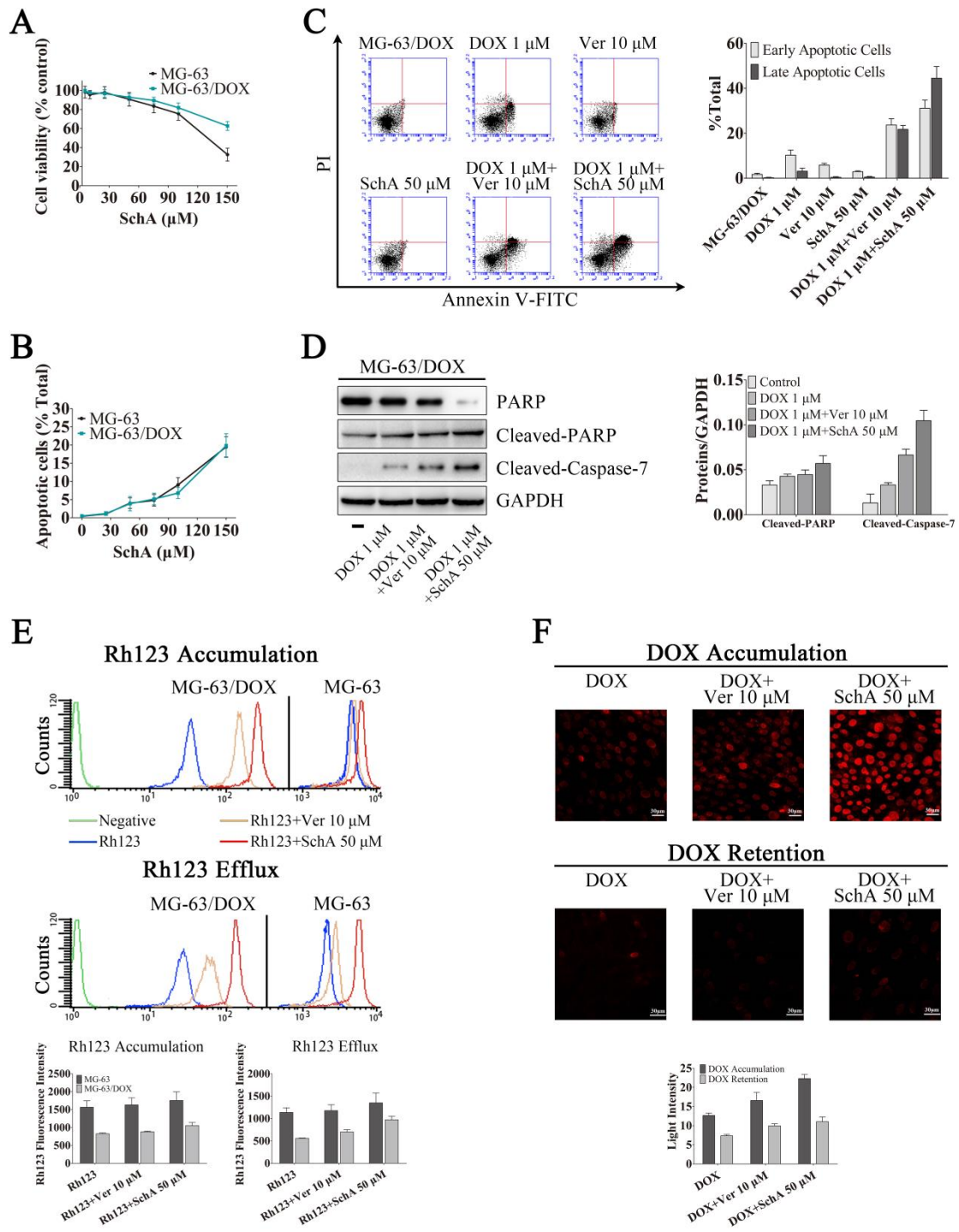


Fig. 3.

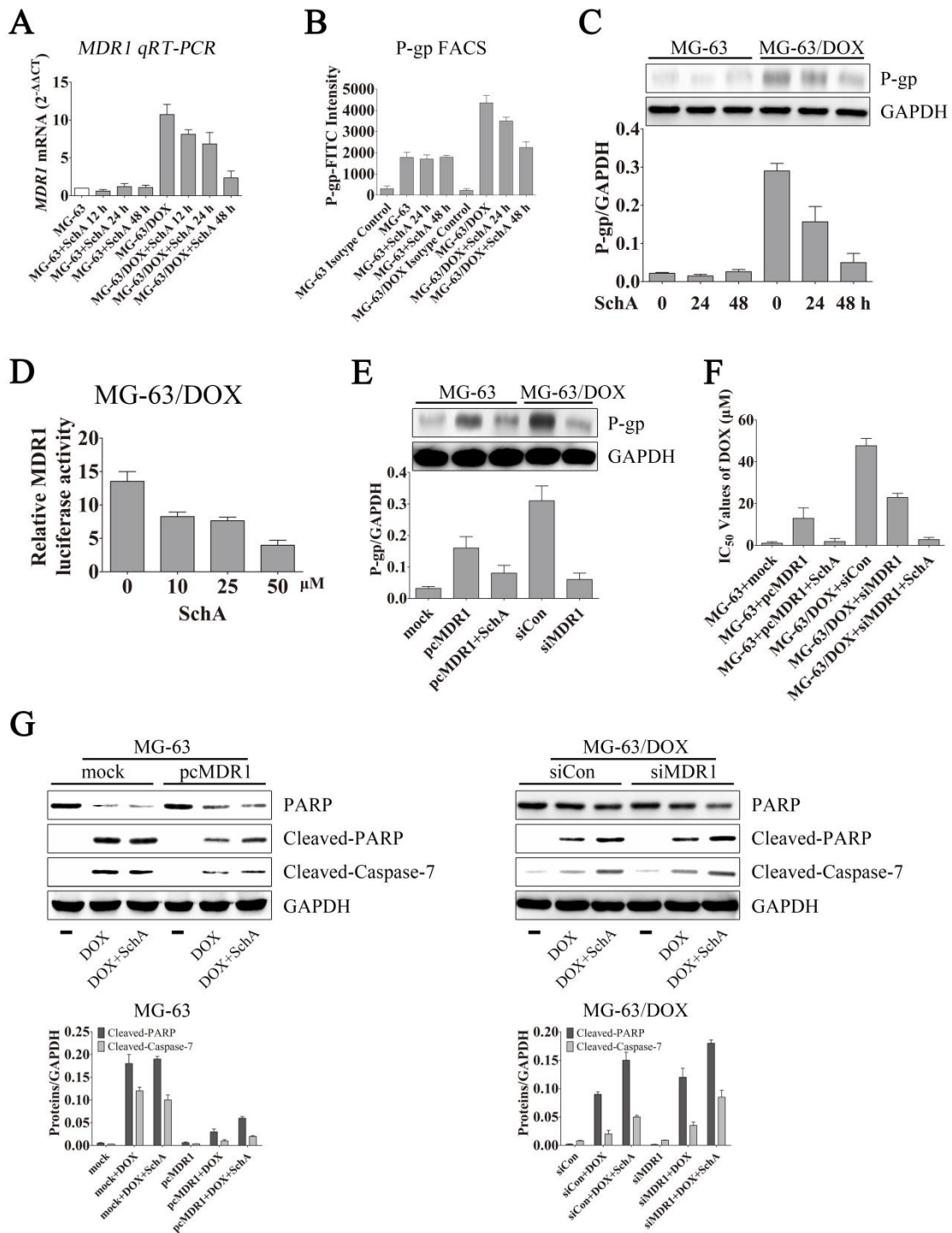


Fig. 4.

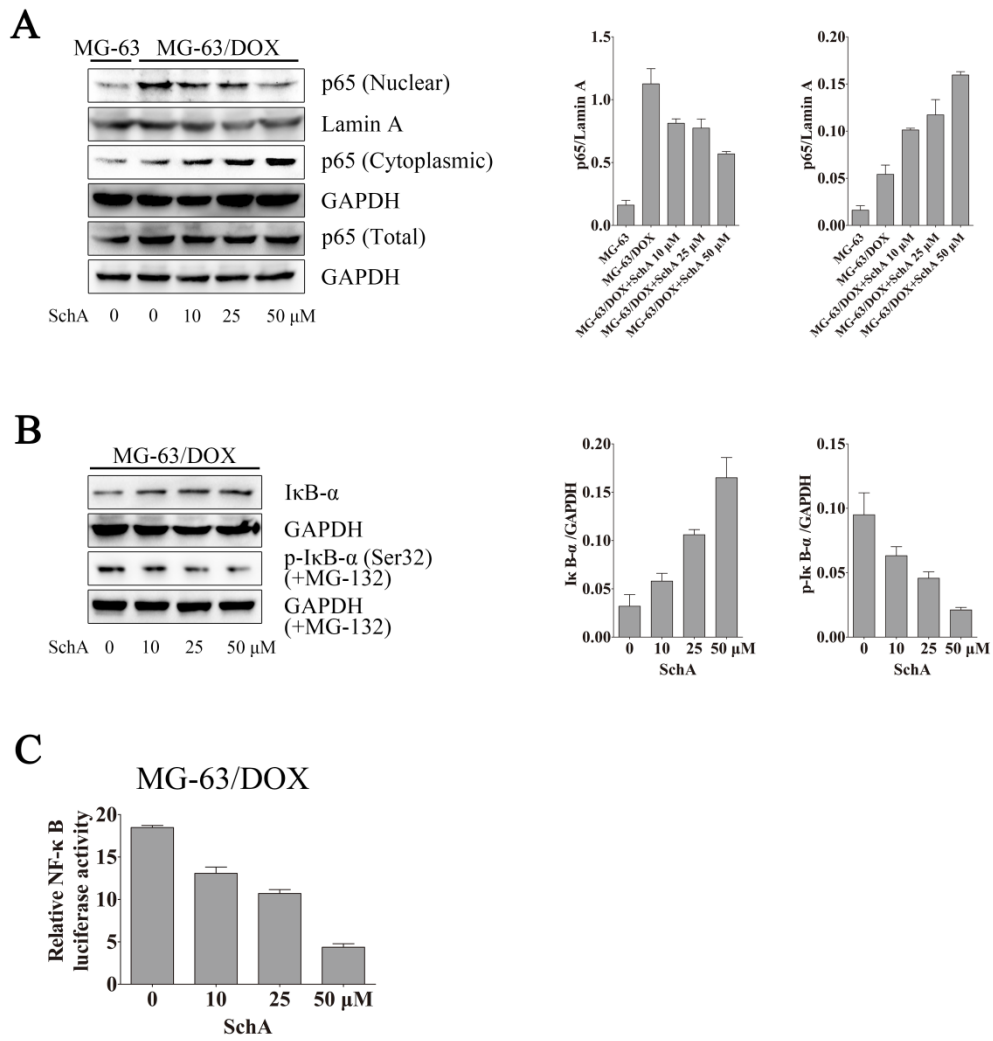


Fig. 5.

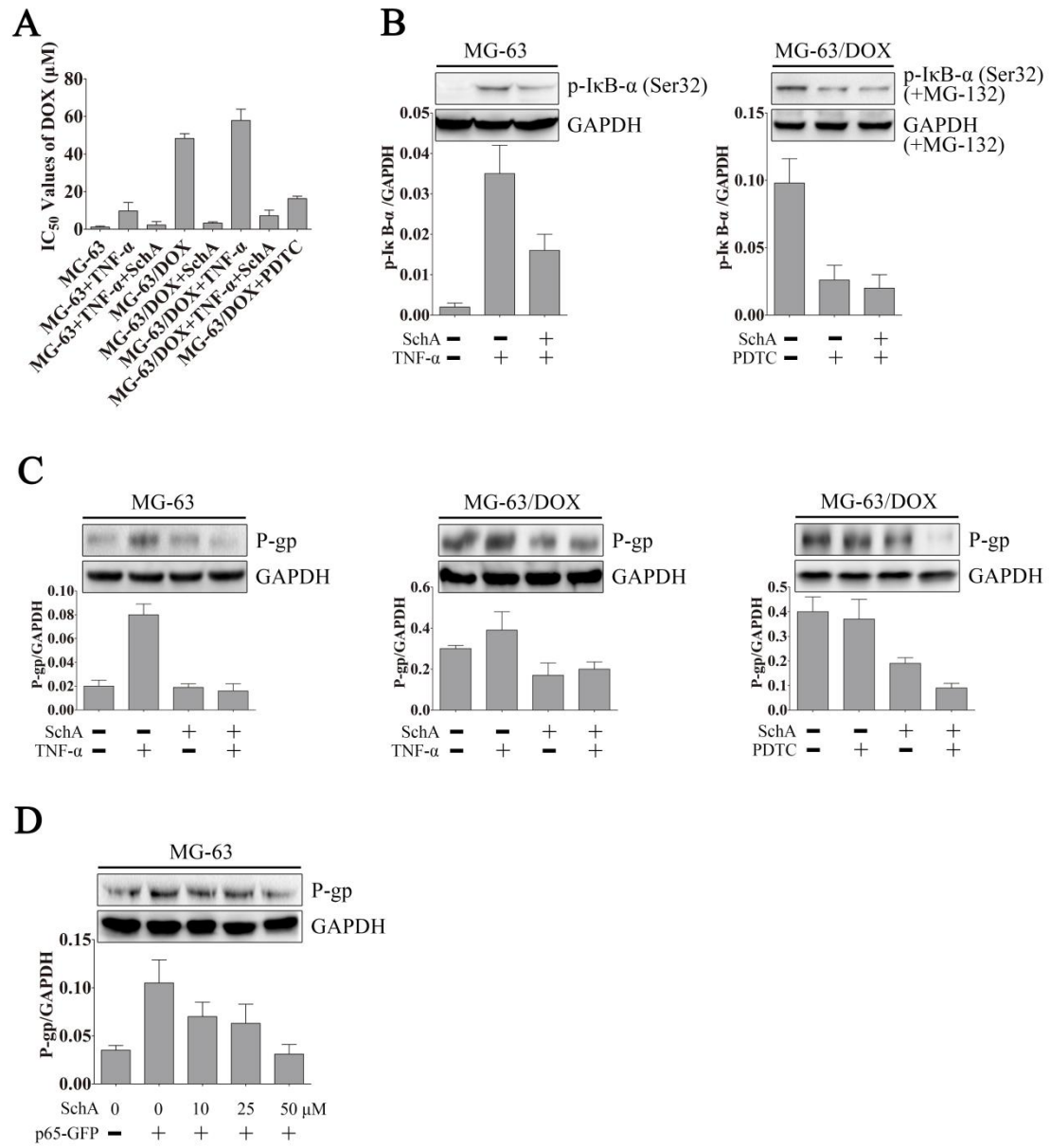


Fig. 6.

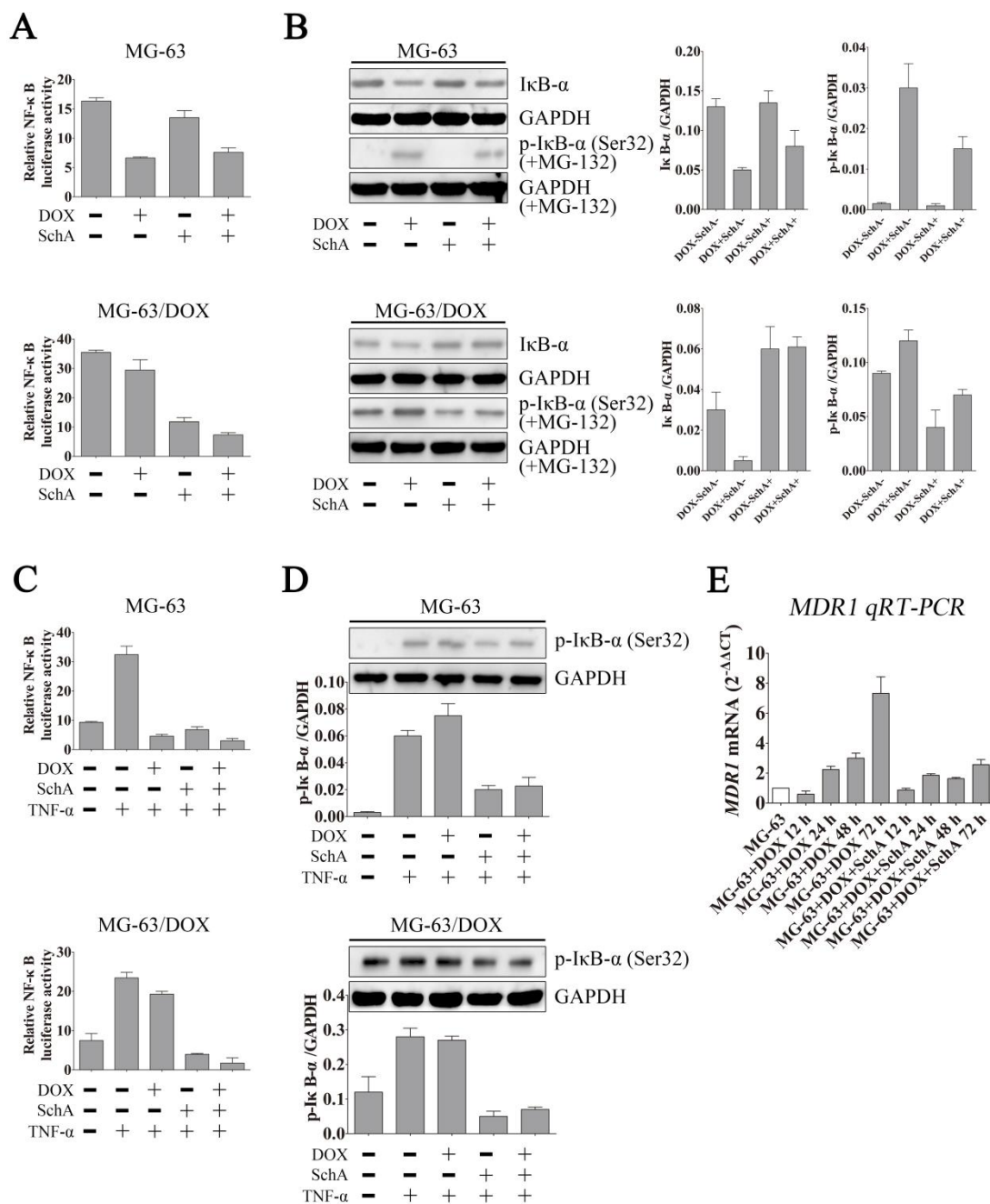


Fig. 7.

Figure legends

Fig. 1 Chemical structure and molecular weight of SchA.

Fig. 2 The DOX resistant subline MG-63/DOX was established and SchA showed an anti-MDR effect. (A) MG-63 or MG-63/DOX cells were seeded into 96-well culture plates and incubated for 1–7 days respectively. MTT assay was performed to measure the cell growth curve. (B) A full range of concentrations of DOX with or without SchA (10–50 μM , 48 h) or Ver (10 μM , 48 h) were added to the MG-63 or MG-63/DOX cells. The IC_{50} values of DOX were measured by the MTT assay. Data are expressed as “means \pm S.D.”.

Fig. 3 SchA enhanced the cytotoxicity of DOX in MG-63/DOX cells by increasing DOX accumulation. (A) MG-63 or MG-63/DOX cells were incubated with 5–150 μM SchA for 48 h. The cell viability was measured by the MTT assay. (B) MG-63 or MG-63/DOX cells were incubated with 0–150 μM SchA for 48 h. The AV-FITC/PI double staining assay was used to analyze the SchA induced apoptosis (early apoptosis plus late apoptosis) detected by flow cytometry. (C) MG-63/DOX cells were maintained in medium containing 1 μM DOX with or without 50 μM SchA or 10 μM Ver for 48 h. The AV-FITC/PI double staining assay was used to analyze the DOX induced apoptosis detected by flow cytometry. Early apoptosis: AV positive but PI negative; Late apoptosis: AV positive and PI positive. (D) Western blot results of the whole-cell lysates. MG-63/DOX cells treated with or without 1 μM DOX combined with or

without 50 μM SchA or 10 μM Ver for 48 h for the detection of cleaved caspase-7 and cleaved PARP with GAPDH as loading control. (E) In the Rh123 accumulation assay, MG-63 or MG-63/DOX cells were pretreated with or without 50 μM SchA or 10 μM Ver for 1 h and then incubated with 5 μM Rh123 in the dark for 1 h. In the Rh123 efflux assay, MG-63 or MG-63/DOX cells were first cultured with 5 μM Rh123 in the dark for 1.5 h, washed three times with warm culture medium, and then incubated in the absence or presence of 50 μM SchA or 10 μM Ver for 1.5 h. Intracellular fluorescence of Rh123 was detected by flow cytometry. (F) In the DOX accumulation assay, MG-63/DOX cells were incubated for 24 h in a medium containing 5 μM DOX with or without 50 μM SchA or 10 μM Ver, washed three times with PBS and fixed in 4% paraformaldehyde for 10 mins at 25°C, then washed three times with PBS and examined for the fluorescence of intracellular DOX. In the DOX retention assay, MG-63/DOX cells were incubated for 24 h in a medium containing 5 μM DOX, and then washed with warm culture medium three times. The cells were incubated for 24 h in a medium with or without 50 μM SchA or 10 μM Ver. Subsequently, the cells were washed three times with PBS and fixed in 4% paraformaldehyde for 10 mins at 25°C, then washed three times with PBS and examined for the fluorescence of intracellular DOX by laser scanning confocal microscopy. Data are expressed as “means \pm S.D.”.

Fig. 4 SchA reverses MDR by inhibiting P-gp expression in MG-63/DOX cells. (A) MG-63 and MG-63/DOX cells were treated with 50 μ M SchA for 0–48 h. *MDR1* mRNA levels were detected by qRT-PCR. The Δ cycle threshold method was used for the calculation of relative differences in mRNA abundance. Data were normalized to the expression of *GAPDH*. The results of real-time RT-PCR were expressed as fold-changes. The normalized value of the target mRNA of the control group is arbitrarily presented as 1. (B) MG-63 and MG-63/DOX cells were treated with 50 μ M SchA for 0–48 h. The expression of P-gp at the membrane surface was analyzed by flow cytometry. (C) Western blot results of the membrane lysates from the MG-63 and MG-63/DOX cells treated with 50 μ M SchA for 0–48 h. (D) MG-63/DOX cells were co-transfected transiently with the human MDR1 luciferase reporter plasmid and the pRL-SV40 plasmid and 36 h later were treated with 0–50 μ M SchA for 8 h prior to harvesting. (E) MG-63 cells were transfected the *MDR1* plasmid or a mock plasmid for 48 h, and treated with or without 50 μ M SchA for 48 h. MG-63/DOX cells were transfected siMDR1 or siCon for 48 h. Western blot analysis was performed. (F) MG-63 cells were transfected with the *MDR1* plasmid or a mock plasmid, and MG-63/DOX cells were transfected with siMDR1 or siCon for 48 h and then incubated with serial dilutions of DOX in the absence or presence of 50 μ M SchA

for another 48 h, follow by the MTT assay. (G) MG-63 cells were transfected with the *MDR1* plasmid or a mock plasmid, and MG-63/DOX cells were transfected with siMDR1 or siCon for 48 h and then incubated with 1 μ M DOX in the absence or presence of 50 μ M SchA for another 48 h, follow by Western blot analysis for the detection of cleaved caspase-7 and cleaved PARP with GAPDH as loading control. Data are expressed as “means \pm S.D.”.

Fig. 5 SchA inhibits NF- κ B signaling in an IKK-dependent manner in MG-63/DOX cells. (A) Western blot results of the nuclear lysates, the cytoplasmic lysates or the whole-cell lysates from the MG-63/DOX cells treated with 0-50 μ M SchA for 24 h, with the MG-63 as negative control. (B) Western blot results of the whole-cell lysates from the MG-63/DOX cells treated with 0-50 μ M SchA or 12 h. Where indicated, cells were also treated with the proteasome inhibitor MG-132 (10 μ M). (C) MG-63/DOX cells were co-transfected transiently with the NF- κ B luciferase reporter plasmid and the pRL-SV40 plasmid and 36 h later were treated with 0-50 μ M SchA for 8 h prior to harvesting. Data are expressed as “means \pm S.D.”.

Fig. 6 SchA reduces P-gp by inhibiting NF- κ B signaling. (A) MG-63 or MG-63/DOX cells were treated with serial dilutions of DOX with or

without 20 μM PDTC or 50 μM SchA and/or 5 nM TNF- α for 48 h, followed by the MTT assay. (B) Western blot results of the whole-cell lysates from the MG-63 cells treated with or without 50 μM SchA for 12 h and/or 5 nM TNF- α for 0.5 h, and the MG-63/DOX cells treated with or without 20 μM PDTC for 1.5 h in the absence or presence of 50 μM SchA for 12 h. Where indicated, cells were also treated with the proteasome inhibitor MG-132 (10 μM). (C) Western blot results of the membrane lysates from the MG-63 and MG-63/DOX cells treated with or without 5 nM TNF- α and/or 50 μM SchA for 24 h, and the MG-63/DOX cells treated with or without 20 μM PDTC for 1.5 h and/or 50 μM SchA for 24 h. (D) MG-63 cells were transfected transiently with or without 10 μg p65-GFP plasmid, and after 48 h were treated with 0–50 μM SchA for 48 h; the membrane lysates were followed by Western blot analysis. Data are expressed as “means \pm S.D.”.

Fig. 7 SchA suppressed DOX-induced I κ B- α phosphorylation and enhanced the inhibitory effect of DOX on NF- κ B transcriptional activity. (A) MG-63 or MG-63/DOX cells were co-transfected transiently with the NF- κ B luciferase reporter plasmid and the pRL-SV40 plasmid and 36 h later treated with or without 1 μM DOX and/or 50 μM SchA for 8 h prior to harvesting. (B) Western blot results of the whole-cell lysates from the MG-63 or MG-63/DOX cells treated with or without 1 μM DOX and/or

50 μM SchA for 12 h. Where indicated, cells were also treated with the proteasome inhibitor MG-132 (10 μM). (C) MG-63 or MG-63/DOX cells were co-transfected transiently with the NF- κB luciferase reporter plasmid and the pRL-SV40 plasmid and 36 h later stimulated for 8 h with or without 1 μM DOX and/or 50 μM SchA and 4 h with 5 nM TNF- α . (D) Western blot results of the whole-cell lysates from the MG-63 or MG-63/DOX cells treated with 1 μM DOX and/or 50 μM SchA for 12 h and 5 nM TNF- α for 0.5 h. (E) MG-63 cells were treated with or without 1 μM DOX for 0–72 h in the absence or presence of 50 μM SchA. *MDR1* mRNA levels were detected by qRT-PCR. The Δ cycle threshold method was used for the calculation of relative differences in mRNA abundance. Data were normalized to the expression of *GAPDH*. The results of real-time RT-PCR were expressed as fold-changes. The normalized value of the target mRNA of the control group is arbitrarily presented as 1. Data are expressed as “means \pm S.D.”.